Electronic Supplementary Material (ESI) for Nanoscale.

Electronic Supplementary Information

Grating-coupled surface plasmon resonance enhanced organic photovoltaic devices induced by Blu-ray disc recordable and Blu-ray disc grating structures

Supeera Nootchanat,[a, b] Apichat Pangdam,[a, b] Ryousuke Ishikawa,[a] Kanet Wongravee,[b] Kazunari Shinbo,[a] Keizo Kato,[a] Futao Kaneko,[a] Sanong Ekgasit,[b*] and Akira Baba[a*]

[a]Graduate School of Science and Technology, Niigata University, 8050, Ikarashi 2-nocho, Nishi-ku, Niigata 950-2181, Japan.

E-mail: ababa@eng.niigata-u.ac.jp

[b] Sensor Research Unit, Department of Chemistry, Faculty of Science, Chulalongkorn University, Bangkok 10330, Thailand.

E-mail: sanong.e@chula.ac.th

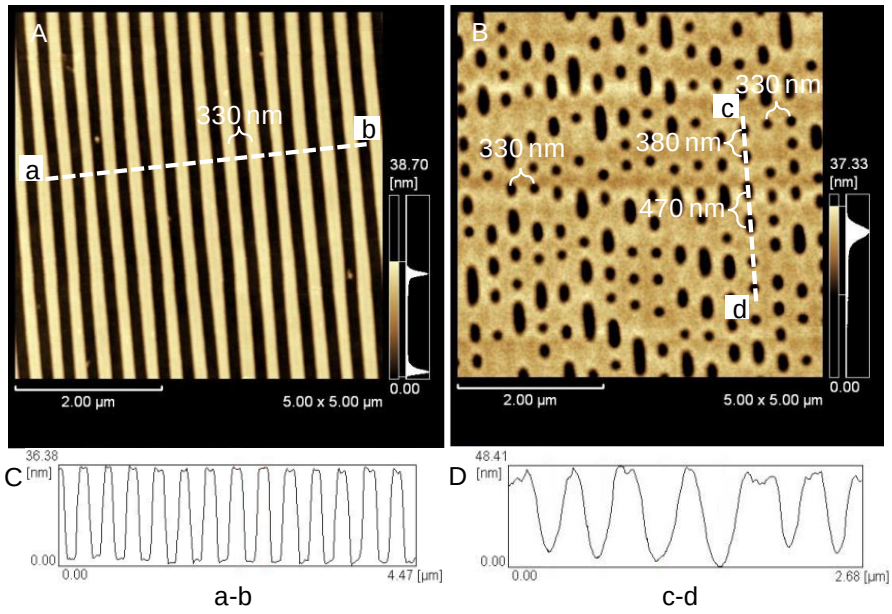

Fig. S1 AFM images showing the cleaned surfaces of the (A) BD-R and (B) BD master templates. Cross-section profiles of (C) BD-R and (D) BD corresponding to lines a–b and c–d in (A) and (B), respectively.

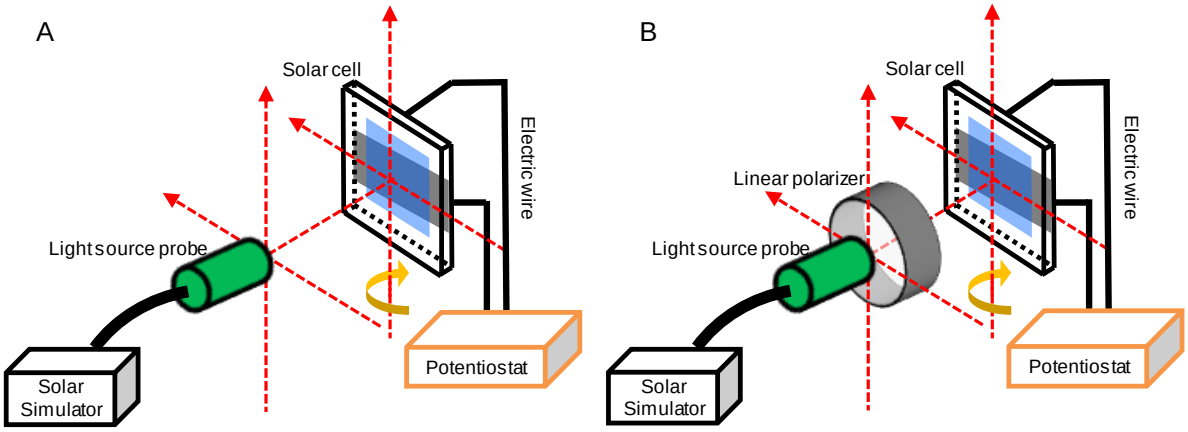

Fig. S2 Photocurrent measurement apparatus for OSCs under irradiation of (A) non-polarized and (B) polarized light.

.

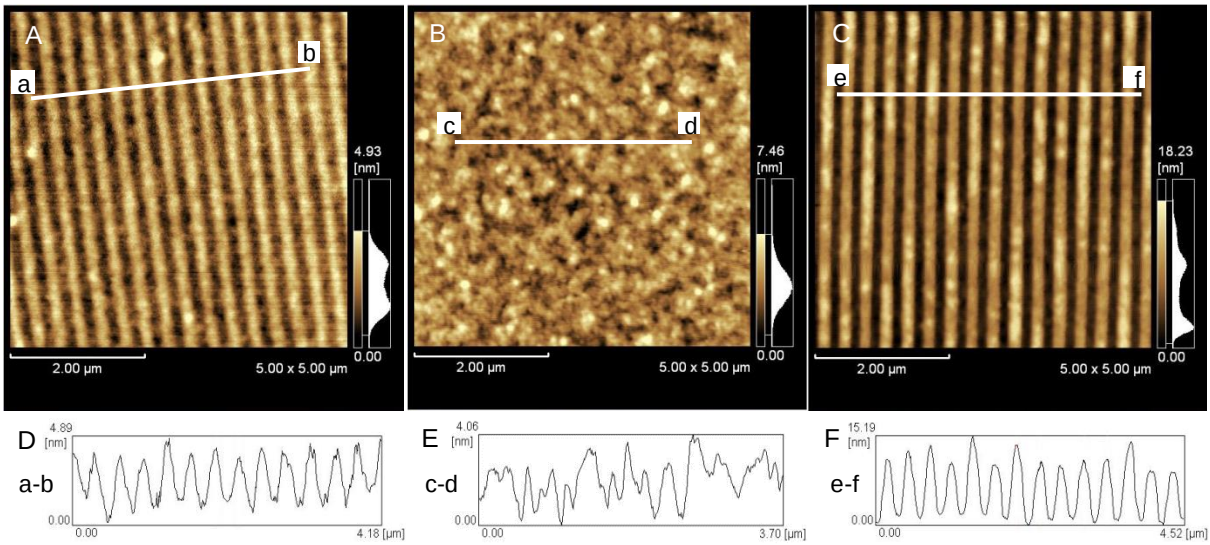

Fig. S3 AFM images showing the surface morphology of P3HT:PCBM films after nanoimprinting of BD-R pattern for imprinting on a (A) damp film without thermal annealing, (B) dried film without thermal annealing, and (C) dried film with thermal annealing at 100 °C. Each imprinting was formed for 30 min after attachment of the BD-R mold.

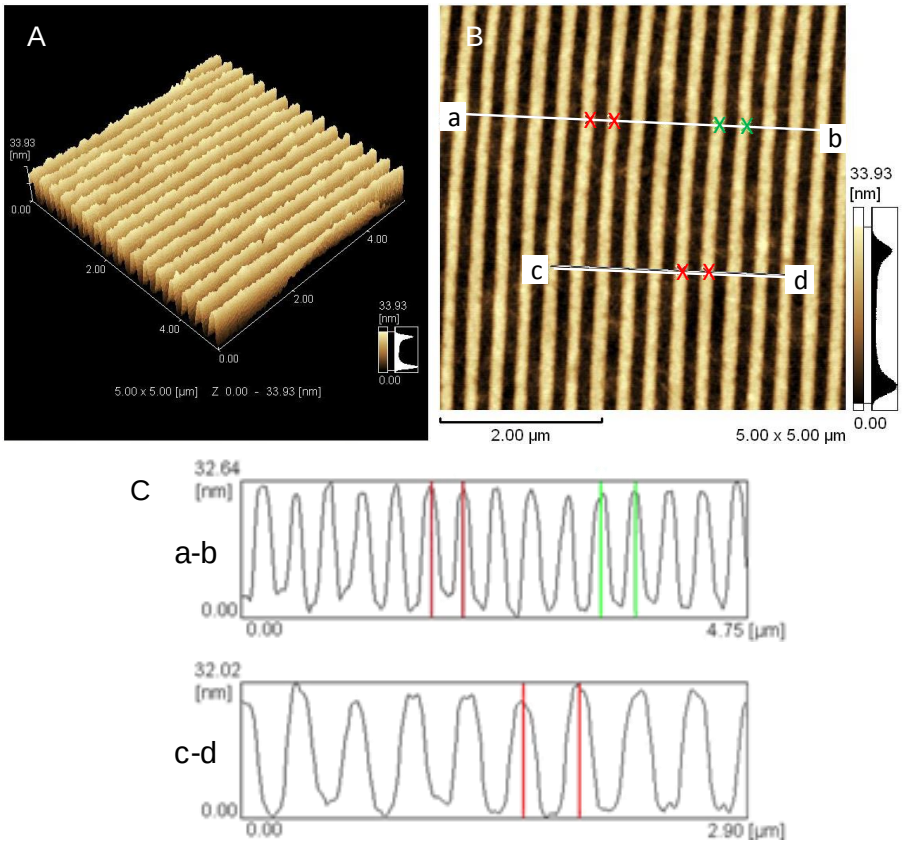

Fig. S4 (A) 3D AFM image, (B) AFM image, and (C) cross-sectional profiles showing the morphology of the BD-R grating pattern on the surface of the P3HT:PCBM layer of a fabricated solar cell.

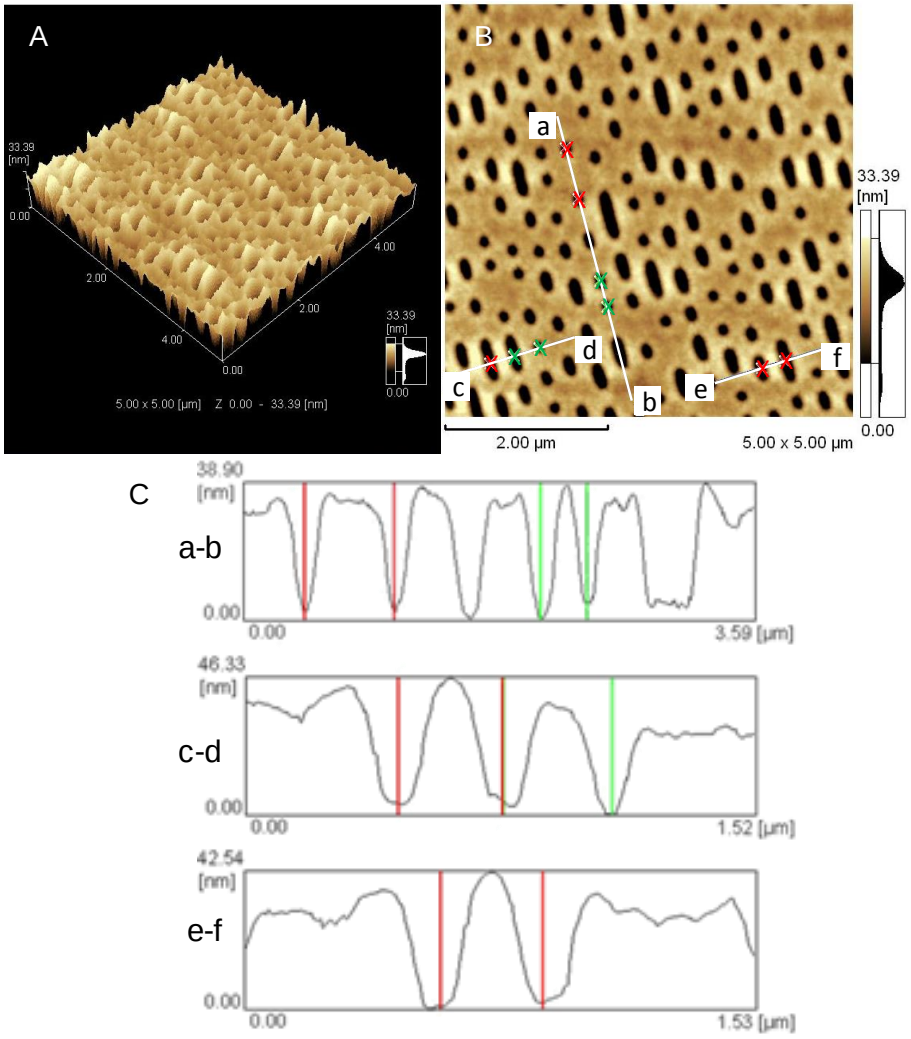

Fig. S5 3D AFM micrograph, (B) AFM micrograph, and (C) corresponding AFM line profiles showing the morphology of the BD grating pattern on the surface of the P3HT:PCBM layer of a fabricated solar cell.

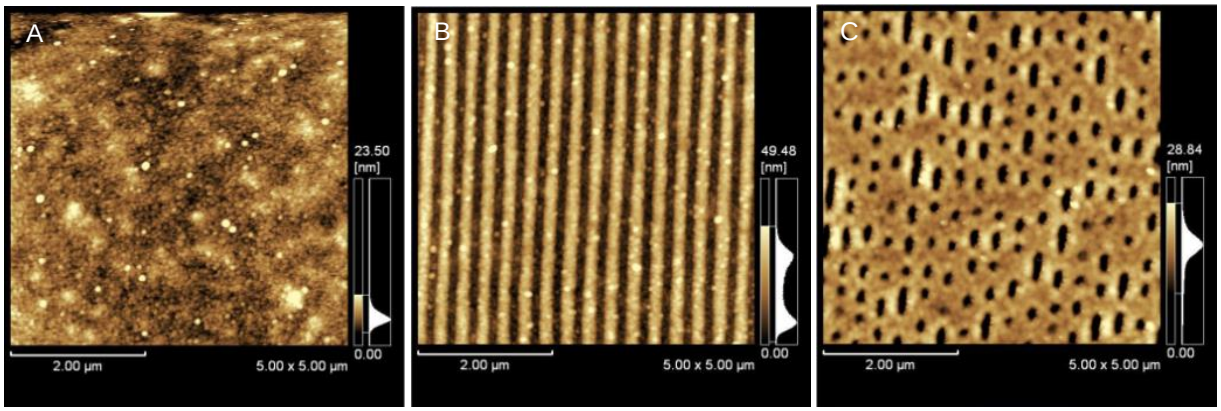

Fig. S6 AFM images showing the surface morphology of the aluminum electrodes of a (A) flat solar cell, (B) BD-R solar cell, and (C) BD solar cell.

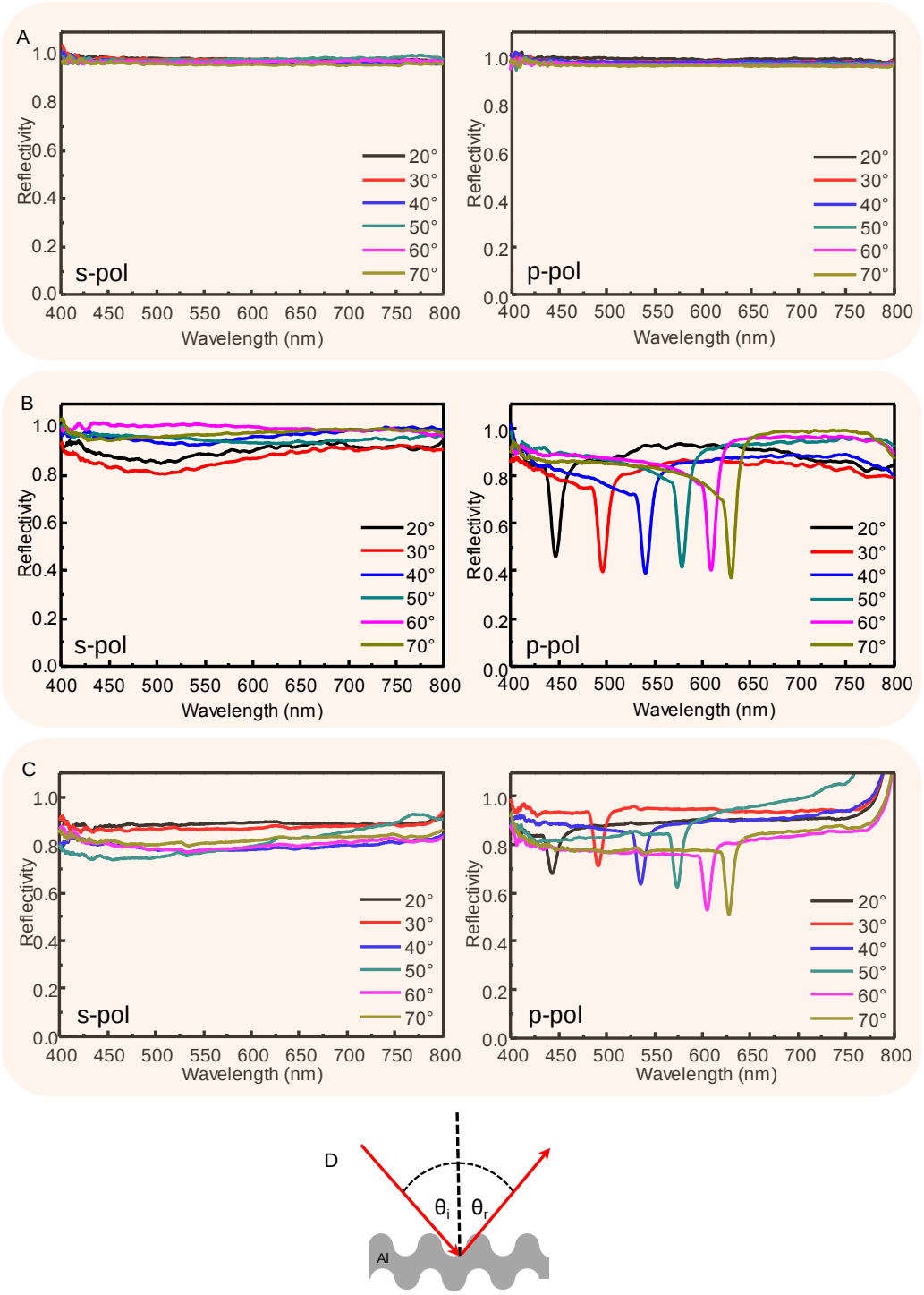

Fig. S7 Reflectivity curves of (A) flat aluminum film, (B) aluminum-coated BD-R grating, and (C) aluminum-coated BD grating at various incident angles. The reflectivity curves were measured under illumination of s- and p-polarized light. (D) Schematic illustrating the light reflection on the textured aluminum films.

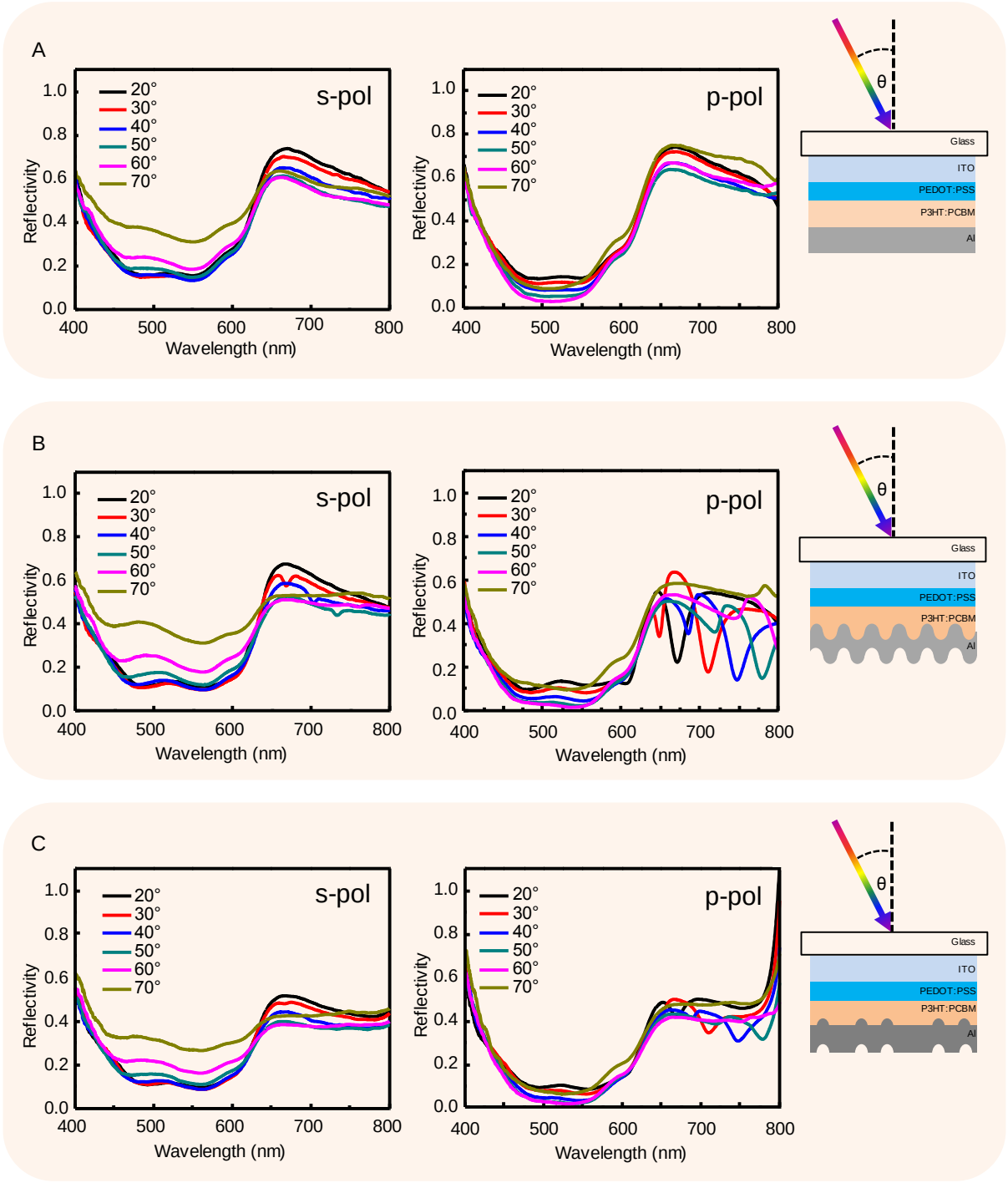

Fig. S8 Reflectivity curves and corresponding schematic of (A) flat solar cell, (B) BD-R solar cell, and (C) BD solar cell. The reflectivity curves were measured at various incident angles under illumination of s- and p-polarized light. (D) Schematic illustrating the light reflection on the textured aluminum films.

Table S1 **E**lectrical parameters of the fabricated OSCs J_{sc}, V_{oc}, PCE, and FF. The electrical parameters were determined from *J*–*V* characterization under an illumination intensity of 75 mW/cm^2 at normal incident angle.

Device	J_{sc} (mA/cm^2)	V_{oc}(vol)	PCE (%)	FF (%)
Flat	6.07±0.17	0.59±0.02	2.49±0.22	0.54±0.04
BD-R	6.68±0.05	0.60±0.02	2.97±0.20	0.57±0.03
BD	6.41±0.21	0.60±0.01	2.57±0.19	0.50±0.04

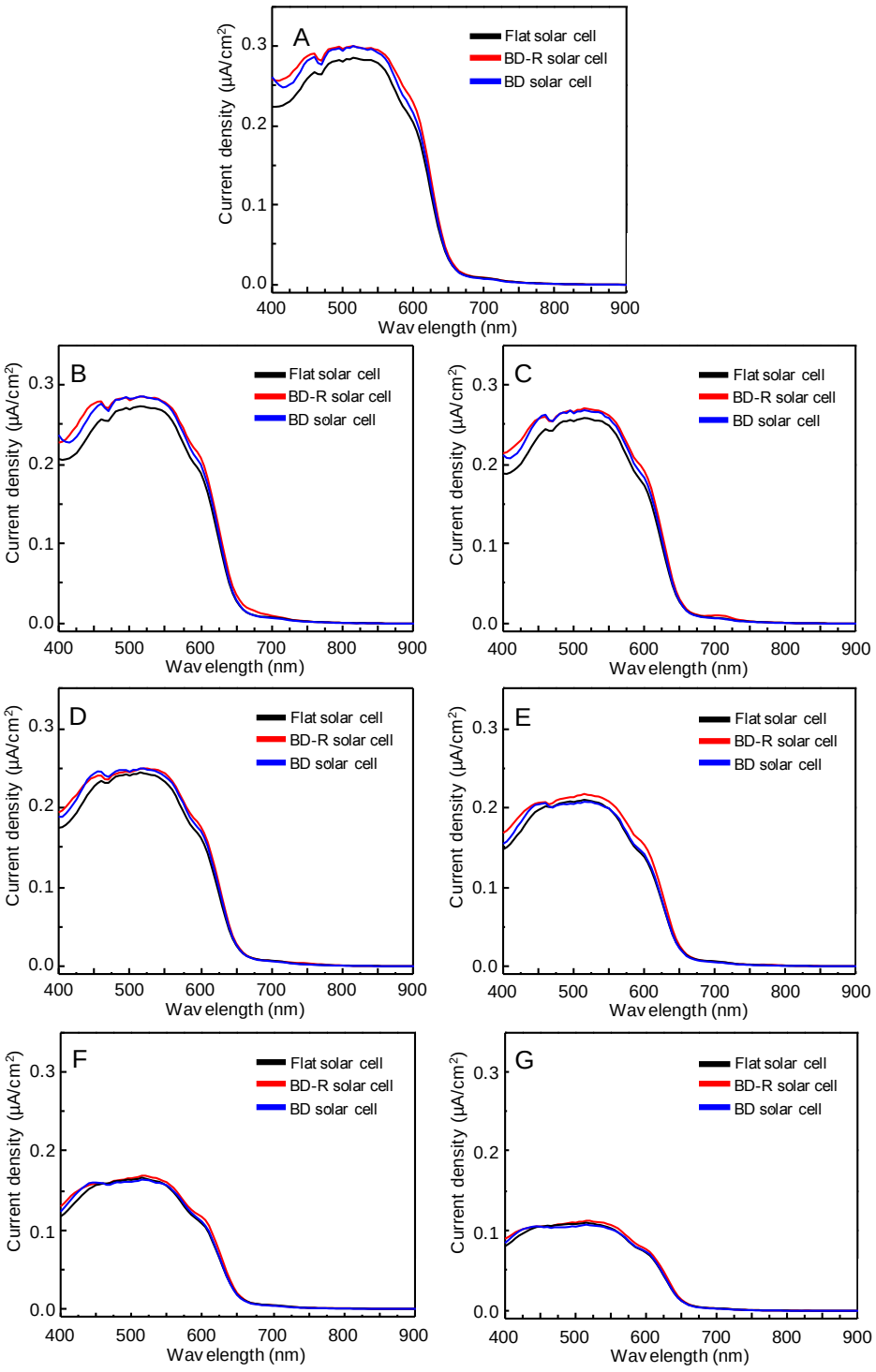

Fig. S9 **S**pectral photocurrent properties of the fabricated solar cells collected at incident angles of (A) 0°, (B) 20°, (C) 30°, (D) 40°, (E) 50°, (F) 60°, and (G) 70°.

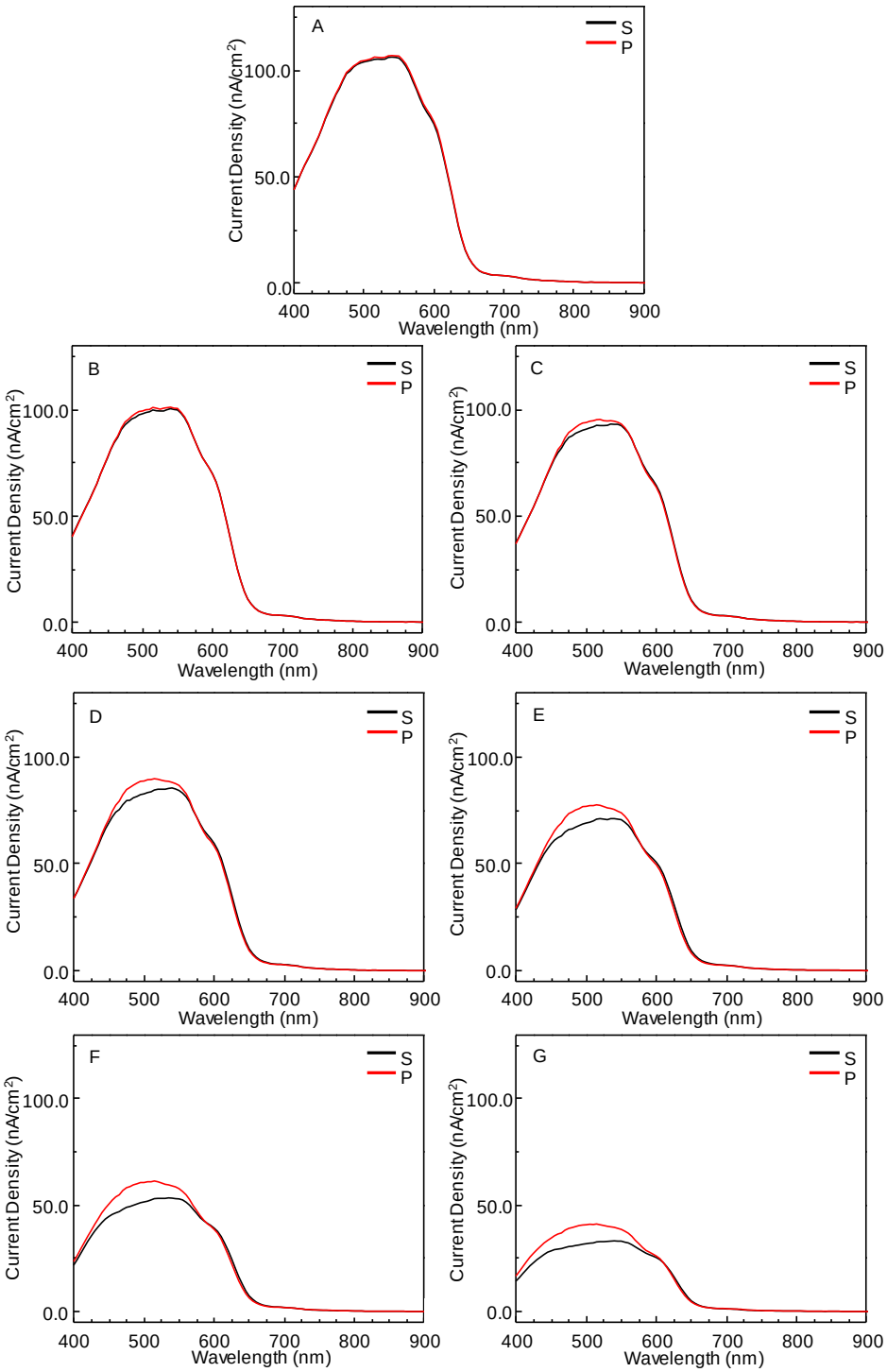

Fig. S10 **S**pectral photocurrent spectra of a flat OSC collected at incident angles of (A) 0°, (B) 20°, (C) 30°, (D) 40°, (E) 50°, (F) 60°, and (G) 70°. The spectral photocurrent spectra were recorded under illumination of polarized light.

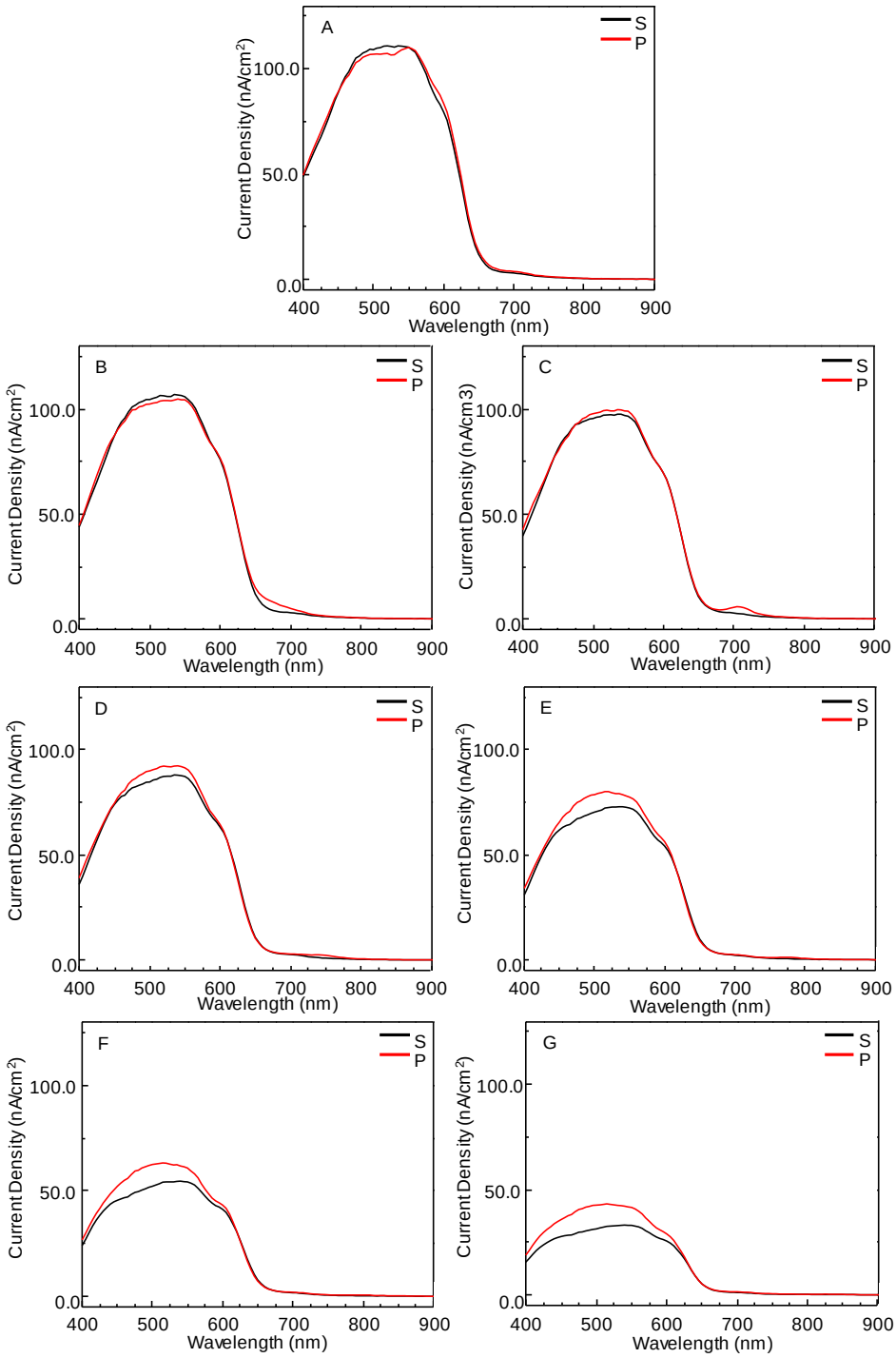

Fig. S11 **S**pectral photocurrent spectra of a BD-R OSC collected at incident angles of (A) 0°, (B) 20°, (C) 30°, (D) 40°, (E) 50°, (F) 60°, and (G) 70°. The spectral photocurrent spectra were recorded under illumination of polarized light.

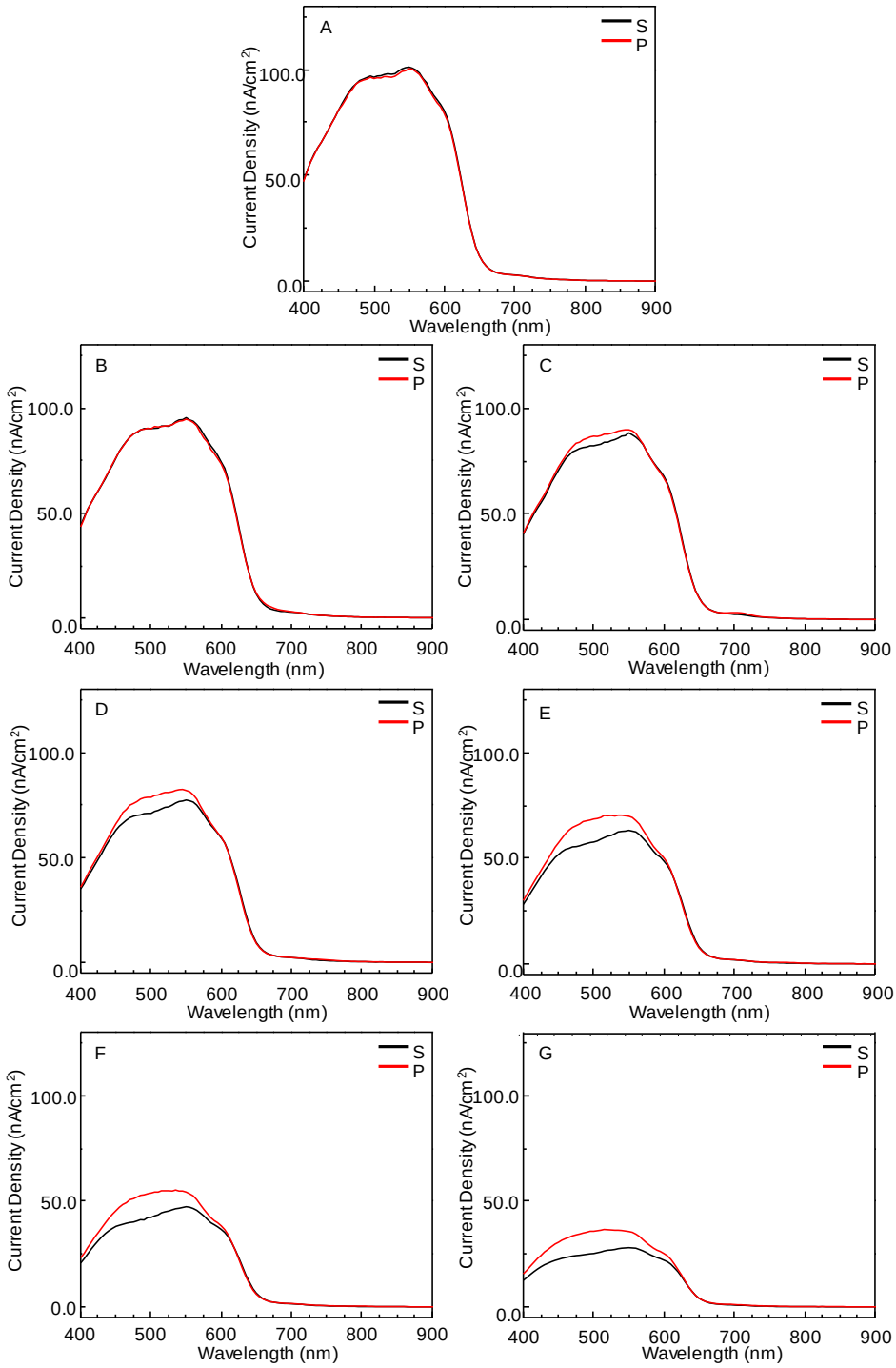

Fig. S12 **S**pectral photocurrent spectra of a BD OSC collected at incident angles of (A) 0°, (B) 20°, (C) 30°, (D) 40°, (E) 50°, (F) 60°, and (G) 70°. The spectral photocurrent spectra were recorded under illumination of polarized light.

Table S2 J_{sc} of the fabricated OSCs under irradiation of s-pol light. The illumination intensity was 75 mW/cm^2.

Incident angle	J_{sc} (mA/cm^2)			improvement of J_{sc} (mA/cm^2)	
	Flat OSC	BD-R OSC	BD OSC	BD-R OSC	BD OSC
0	3.89	4.23	4.06	**0.34 (8.74 %)**	**0.17 (4.33)**
20	3.73	4.01	3.83	**0.28 (7.49 %)**	**0.10 (2.67)**
30	3.54	3.73	3.58	**0.20 (5.56 %)**	**0.04 (1.08)**
40	3.23	3.36	3.20	**0.13 (3.92 %)**	**-0.03 (-0.85)**
50	2.80	2.86	2.70	**0.06 (2.08 %)**	**-0.10 (-3.61)**
60	2.22	2.23	2.04	**0.01 (0.61 %)**	**-0.17 (-7.78)**
70	1.49	1.42	1.28	**-0.07 (-4.93 %)**	**-0.21 (-14.16)**

Table S3 J_{sc} of the fabricated OSCs under irradiation of p-pol light. The illumination intensity was 75 mW/cm^2.

Incident angle	J_{sc} (mA/cm^2)			improvement of J_{sc} (mA/cm^2)	
	Flat OSC	BD-R OSC	BD OSC	BD-R OSC	BD OSC
0	3.88	4.29	4.05	**0.41 (10.53 %)**	**0.17 (4.26 %)**
20	3.74	4.11	3.86	**0.37 (9.94 %)**	**0.12 (3.18 %)**
30	3.57	3.86	3.65	**0.29 (8.21 %)**	**0.08 (2.26 %)**
40	3.30	3.52	3.33	**0.22 (6.69 %)**	**0.03 (0.94 %)**
50	2.92	3.11	2.89	**0.19 (6.51 %)**	**-0.04 (-1.22 %)**
60	2.39	2.55	2.29	**0.16 (6.63 %)**	**-0.10 (-4.10 %)**
70	1.70	1.76	1.56	**0.05 (3.16 %)**	**-0.14 (-8.13 %)**